Revista Mexicana de Física
ISSN: 0035-001X
rmf@ciencias.unam.mx
Sociedad Mexicana de Física A.C.
México

Leal-Cruz, A.L.; Pech-Canul, M.I.; de la Peña, J.L.
A low-temperature and seedless method for producing hydrogen-free Si3N4
Revista Mexicana de Física, vol. 54, núm. 3, junio, 2008, pp. 200-207
Sociedad Mexicana de Física A.C.
Distrito Federal, México

A low-temperature and seedless method for producing hydrogen-free Si_3N_4

A.L. Leal-Cruz, M.I. Pech-Canul*, and J.L. de la Peña
Centro de Investigación y de Estudios Avanzados del IPN-Unidad Saltillo,
Carr. Saltillo-Monterrey Km. 13. Saltillo, 25900 Coahuila, México.

Recibido el 17 de septiembre de 2007; aceptado el 3 de abril de 2008

A simple, seedless method for the synthesis of Si_3N_4 from a hydrogen-free precursor system ($Na_2SiF_{6(s)}$-$N_{2(g)}$) was developed. From thermodynamic calculations and experimental results it is concluded that the gaseous chemical species SiF_x (SiF_4,SiF_3, SiF_2, SiF and Si) formed during the low-temperature dissociation of Na_2SiF_6 in a conventional CVD system react *in-situ* with nitrogen to produce Si_3N_4. Whiskers, fibers, coatings and powders were obtained via the Na_2SiF_6-N_2 system at pressures slightly above atmospheric pressure. Not only does the feasibility of the reactions for Na_2SiF_6 dissociation and Si_3N_4 formation increase with the temperature but also, once the SiF_x chemical species are formed by the former, the latter reaction is even more viable. Amorphous Si_3N_4 is obtained at temperatures of up to 1173 K while crystalline α- and β-Si_3N_4 are formed in the range 1273-1573 K and with processing times as short as 120 minutes. Optimal conditions for maximizing Si_3N_4formation were determined.

Keywords: Thermodynamics; CVD; Amorphous Si_3N_4; α- and β-Si_3N_4; gas-solid precursors.

Se desarrolló un método simple y sin semillas para la síntesis de Si_3N_4 partiendo de un sistema de precursores libre de hidrógeno ($Na_2SiF_{6(s)}$-$N_{2(g)}$). A partir de cálculos termodinámicos y resultados experimentales se concluye que las especies químicas gaseosas SiF_x (SiF_4,SiF_3, SiF_2, SiF and Si) formadas durante la disociación a baja temperatura del Na_2SiF_6 en un sistema convencional de CVD reaccionan in situ con el nitrógeno para producir Si_3N_4. Se obtuvieron fibras, fibras cortas discontinuas, recubrimientos y polvos a través del sistema $Na_2SiF_{6(s)}$-N_2 a presiones ligeramente por encima de la presión atmosférica. Con el incremento en la temperatura no solo aumenta la factibilidad de las reacciones para la disociación del Na_2SiF_6 y formación del Si_3N_4, sino también una vez que se han formado las especies SiF_x por la primera reacción, la segunda reacción es incluso más factible. El Si_3N_4 amorfo se obtiene a temperaturas de hasta 1173 K mientras que el Si_3N_4 cristalino α y β se forman en el rango de temperaturas de 1273-1573 K y con tiempos de procesamiento tan cortos como 120 minutos. Se determinaron las condiciones óptimas para maximizar la formación del Si_3N_4.

Descriptores: Termodinámica; CVD; Si_3N_4amorfo; $Si_3N_4\alpha$ y β; precursores gas-sólido.

PACS: 81.15.Gh; 81.20.Ka; 82.60.-s

1. Introduction

As a consequence of the increasing demand for silicon nitride (Si_3N_4) both for structural and functional applications although it has been under investigation since the 1960's-70's, a considerable number of new or alternative synthesis methods have been proposed over the past 20 years [1-12]. In addition to the former interest in this ceramic material for structural applications, the synthesis of both amorphous and crystalline Si_3N_4 has been intensively investigated for optoelectronic and microelectronic applications [13-21]. Within the semiconductor industry most of the interest in nitrogen-silicon compounds was particularly as thin films for use as passivation layers to protect semiconductor devices, as gate dielectric layers in thin-film transistors (TFT) and as insulator layers to fabricate metal-nitride-oxide-silicon (MNOS) devices [22]. Also, owing to its excellent physicochemical properties and resistance to the diffusion of impurities, Si_3N_4 was considered as a prominent candidate for substituting silicon dioxide in MOS devices [13]. In addition to low-temperature and cost-effective processing characteristics, especially for electronic applications, it is essential that the silicon nitride thin films have a low hydrogen concentration. This is because, according to previous reports, hydrogen from silane and ammonia used during processing causes film degradation [21].

The synthesis route for amorphous, α- and β-Si_3N_4involving gas phase reactions -commonly referred to as chemical vapor deposition (CVD) - typically starts from silicon gas precursors (silane and halides such as $SiCl_4$, SiF_4, $SiBr_4$ and SiI_4) or silicon liquid precursors (metalorganics as tetra-methyl-silane), and mainly from ammonia as a nitrogen gas precursor [23,24]. During processing, the liquid or gas precursors undergo decomposition into more reactive species that further interact to form Si_3N_4. Silane (SiH_4) and silicon tetrachloride ($SiCl_4$) are the most commonly used silicon precursors while ammonia is the most preferred nitrogen precursor. The reason why NH_3 is preferred over N_2 is because the latter is thermally and chemically more stable than the former, and therefore more difficult to dissociate. Specifically, while the ionization potential for N_2 is 15.576 eV, the corresponding value for NH_3 is 10.2 eV [25]. Consequently, the synthesis of Si_3N_4 using only N_2 (to obtain, accordingly, nitride deposits free of hydrogen), and conventional CVD systems with common silicon precursors has long been a challenging task.

The film contamination issue with hydrogen and the impracticality of using nitrogen in conventional CVD reactors has been addressed from two different perspectives: (1) using hydrogen-free silicon precursors ($SiCl_4$, $SiBr_4$, SiI_4 and SiF_4) and (2) coupling additional devices to standard CVD systems. As regards the first approach, although $SiCl_4$ is

the most frequently used halide, it has been reported that it tends to polymerize and consequently clog the reactor's exit port [26].

With respect to the second approach, the conventional chemical vapor deposition (CVD) system has been modified to plasma assisted CVD, essentially as a means of promoting dissociation of the gas molecules into more reactive radicals, atoms or ions. The most common adaptations include remote enhanced CVD (RECVD), electron cyclotron resonance CVD (ECRCVD) and inductively coupled plasma CVD (ICP-CVD) [13,15,16,19-21,24]. And although plasma-enhanced chemical vapor deposition (PECVD) is the most frequently used technique (in terms of lowering the substrate temperature), it has the disadvantage of potential film degradation by contamination with hydrogen from silane (SiH_4) and ammonia (NH_3) [19].

Recently, a novel synthesis method for Si_3N_4 using a silicon solid precursor was proposed [12]. The method is based on the ability of some solids to form highly reactive chemical species that react with nitrogen-containing precursors (N_2 or N_2-NH_3) in a conventional CVD reactor, taking advantage of the intrinsic thermal gradients within the reactor to produce key reactive chemical species from Na_2SiF_6. Due to its good stability at atmospheric pressure and at room temperature, as well as to its relatively low decomposition temperature ($\approx$ 823 K), Na_2SiF_6 has been considered by several authors for various purposes, other than the synthesis of silicon nitride [27-29]. It should be recognized that in all previous research it was assumed that the only gaseous reaction product formed during the thermal decomposition of $Na_2SiF_6$was silicon tetrafluoride (SiF_4) [27-29]:

$$Na_2SiF_{6(s)} \rightarrow SiF_{4(g)} + 2NaF_{(s)} \quad (1)$$

Since the proposed synthesis method combines the use of gas (N_2, NH_3 and N_2-NH_3mixes) and solid precursors (Na_2SiF_6), it is referred to as a hybrid precursor-based method. Some of the potential benefits of the proposed method [12], with respect to existing commercial and alternative routes, are as follows:

1.- *in situ* processing, because the silicon gas species (SiF_4, SiF_3, SiF_2, SiF and Si) are formed in the same reactor in which $Si_3N_4$is produced,

2.- versatility, because it makes it possible to synthesize Si_3N_4 with a variety of morphologies (whiskers/fibers, films/coatings and particles),

3.- silicon nitride can be produced without the use of seeds of this ceramic material,

4.- economical, because by taking advantage of the intrinsic thermal gradients within the tube reactor, the process makes it possible to save energy,

5.- low-pressure process, because it is carried out at pressures slightly above atmospheric pressure,

6.- since the silicon solid precursor (Na_2SiF_6) is stable and safe at room temperature, it is used as a safe-deposit compound for the silicon gas species,

7.- the process offers the potential of producing Si_3N_4 *in pure nitrogen* in a simple thermal gradient reactor.

The reasons behind the possibility to produce this ceramic in nitrogen only are the subject matter of the present work. In this paper the authors explain in detail why it is possible to produce Si_3N_4 in a simple thermal gradient CVD system using only nitrogen, and propose a mechanism for Na_2SiF_6 dissociation and Si_3N_4formation.

2. Experimental

The experimental work is divided into two parts. The first part corresponds to the optimization of the processing parameters to maximize formation of Si_3N_4 and the second one to the proposition of a mechanism for Na_2SiF_6 dissociation and Si_3N_4 formation in the Na_2SiF_6-N_2 system. Parameter optimization was carried out by means of a Taguchi experimental design and analysis of variance (ANOVA) while the mechanism was proposed on the basis of experimental results and thermodynamic predictions using the FactSage software and databases.

2.1. Apparatus

Figure 1a is a schematic diagram of the experimental set-up used in the study. The reactor consists of a horizontal alumina tube furnace (76.20 cm long $\times$ 3.80 cm in diameter) provided with end-cap fittings to control the process atmosphere. A reactor of this type is characterized by the thermal gradients along the tube's longitudinal direction, as shown through the temperature profile measured in the reactor (see

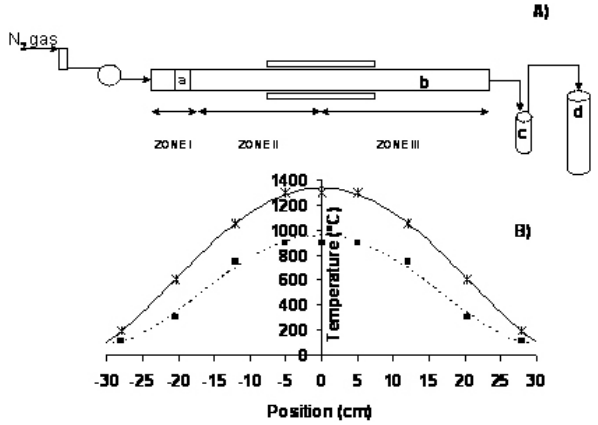

FIGURE 1. Schematic diagram of the experimental set-up indicating position of: (a) solid precursor, (b) substrates, (c) powder collector and (d) neutralizer. (B) Thermal gradients along the reactor longitudinal direction.

Fig. 1b). The thermal gradients are used to strategically induce Na_2SiF_6 (the Si solid precursor) decomposition, stimulate development of the reactions for Si_3N_4 synthesis and heat the substrates for Si_3N_4 deposition. The appropriate temperature range for Na_2SiF_6 decomposition (523-823 K) was determined previously by thermal analysis [30]. The reactor is also provided with gas inlets and outlets to supply the nitrogen precursors as well as to make it possible to remove the gas reaction products (which are made to bubble into distilled water contained in a closed deposit). Two thermocouples placed strategically within the reactor are used to monitor the solid-precursor and substrate temperatures. Gas flow meters and manometers at the reactor entrance and exit ports make it possible to control the processing parameters during the synthesis trials.

2.2. Synthesis and characterization

The synthesis trials were carried out in the conventional CVD reactor described above. In order to investigate the effect of the processing variables on the characteristics of deposited $Si_3N_4$and optimize the processing parameters, a Taguchi experimental design supported by analysis of variance (ANOVA) was used [31]. In the first part of the study, the processing parameters time, temperature, pressure and amount of Na_2SiF_6 were examined at two levels (60 and 120 minutes, 1173 and 1573 K, 17 and 19 mbars, and, 0 and 25 g, correspondingly). Additional tests were carried out at temperatures of 1153, 1303, 1453 and 1606 K each for 0, 35, 70 and 140 min. The Na_2SiF_6compacts were located near the reactor entrance, where the temperature can be varied between 386-578 and 465-873 K and the substrates were placed within the reactor in specific positions where the temperature can be controlled between 1173 and 1573 K, depending on the processing temperature. In this regard, the processing temperature and substrate temperature are two different parameters considered in the experiment. A substrate specimen, however, can be treated at a given processing temperature but at the same time at different substrate temperatures, depending on its position within the reactor. As both Na_2SiF_6 dissociation and Si_3N_4 formation occur in the same reactor, the synthesis route is referred to as an *in situ* process. The substrates consist of SiC_p/Si cylindrical performs (37 mm in diameter $\times$ 25.4 mm long) with 50% porosity prepared by the uniaxial compaction of the corresponding powders, both with an average particle size of 25 μm. As illustrated in Fig. 1, to facilitate the description of the events occurring during synthesis, the reactor was divided into three different zones, namely, Na_2SiF_6 dissociation (Zone I), Si_3N_4formation (Zone II) and Si_3N_4 deposition (Zone III). Once the silicon precursor (Na_2SiF_6) and the substrates were placed in their corresponding positions, the reactor was closed and the system was heated at a rate of 15 °C/min in ultra high purity (UHP) nitrogen to the test temperature, maintained isothermally for the corresponding test time (according to the experimental design) and cooled to room temperature at 15 °C/min. After cooling to room temperature, the substrates were removed from the reactor to determine the amount of Si_3N_4 deposited, as well as for microstructure characterization using Fourier transform infrared spectroscopy (FT-IR), X-ray diffraction (XRD), scanning electron microscopy (SEM) and energy dispersive X-ray spectroscopy (EDX).

Reaction mechanisms for Na_2SiF_6 dissociation and Si_3N_4 formation are proposed on the basis of thermodynamic predictions and experimental results. Accordingly, CVD phase diagrams for the Na_2SiF_6-N_2, SiF_4-N_2, SiF_3-N_2, SiF_2-N_2, and SiF-N_2 systems as well as Ellingham diagrams for the dissociation reaction of $Na_2SiF_6$and for the reaction through which Si_3N_4 is formed were constructed using the FactSage software and databases. FactSage is the fusion of two well-known software packages in the field of computational chemistry: FACT-Win (formerly F*A*C*T) and ChemSage (formerly SOLGASMIX). Phase stability diagrams were constructed graphing absolute temperature (K) *vs.* molar ratio of the silicon precursor divided by the sum of the silicon precursor and nitrogen precursor (for instance, SiF/(SiF+N)). Ellingham diagrams were constructed graphing the Gibbs free energy of the reactions (calculated using FactSage) as a function of temperature. All calculations were carried out at a constant pressure of 1032 mbars (1 atm).

3. Results and discussion

3.1. Optimization of the processing parameters

Analysis of variance provides insight into the optimum process parameters and makes it possible to estimate the percent contribution of each of the parameters tested to the variability in the measured quantities (in this particular case, the amount of Si_3N_4 deposited) [31]. Results from the experimental design considering the variables time, temperature, pressure and amount of Na_2SiF_6showed that this last one is the processing parameter that most significantly influences (with a relative contribution of 99%) the formation of Si_3N_4 and that the effect of the other parameters can be neglected. The amount of Na_2SiF_6 was expected to produce a strong effect on Si_3N_4formation because it supplies the silicon precursor, which is an essential ingredient. This result ultimately substantiates the view that Si_3N_4 is formed via the thermal decomposition of Na_2SiF_6 and not through a conventional nitridation process. In view of this result, as a second approach of the process optimization, only the parameters pressure, temperature and time were considered in the experimental design (setting the amount of Na_2SiF_6 at 25 g). Results from the analysis of variance (ANOVA) are shown in Table I. According to ANOVA, pressure is the parameter with the most significant effect on the amount of Si_3N_4 formed (with a relative contribution of 34%) followed by temperature (31%) and time (31%).The remaining 4% is due to experimental error. Figure 2 is a chart of the main effect of each of the processing parameters tested (at two levels) on the amount of deposited

Si_3N_4 (the response variable). This graph indicates that, although the amount of silicon nitride is enhanced by the second level of temperature, time and amount of Na_2SiF_6, the second level of the latter significantly impacts the magnitude of the response variable. And, although the improvement seems to be irrelevant, it is also clear that it is better to use the lowest level of pressure. Accordingly, the optimum conditions to maximize Si_3N_4 formation from the Na_2SiF_6-N_2 system are: 1573 K, 120 minutes, 17 mbars, and a Na_2SiF_6 compact of 25 g.

TABLE I. ANOVA table for Si_3N_4 formation in the $Na_2SiF_{6(s)}$-$N_{2(g)}$ system.

Parameters	DF	SS	V	F	P(%)
Time	1	0.0105	0.010	0.298	31
Temperature	1	0.0105	0.010	0.298	31
Pressure	1	0.0113	0.011	0.328	34
Error	1	0.0090	0.001	0.001	4
Total	3	0.032	0.032	0.964	100

DF: Degrees of freedom, SS: sum of squares, V: variance, F: Variance ratio, P: Percentage contribution.

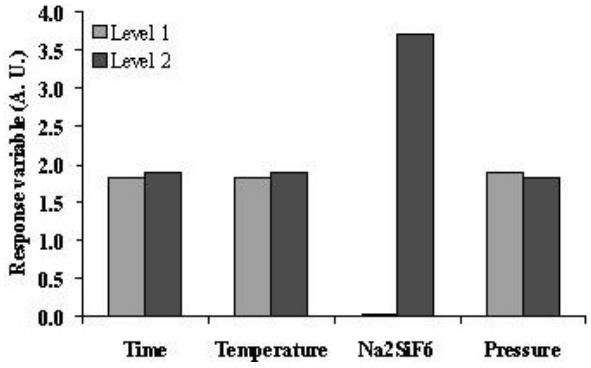

FIGURE 2. Principal effects of independent variables used in the optimization of the processing parameters to maximize the amount of deposited Si_3N_4(the response variable).

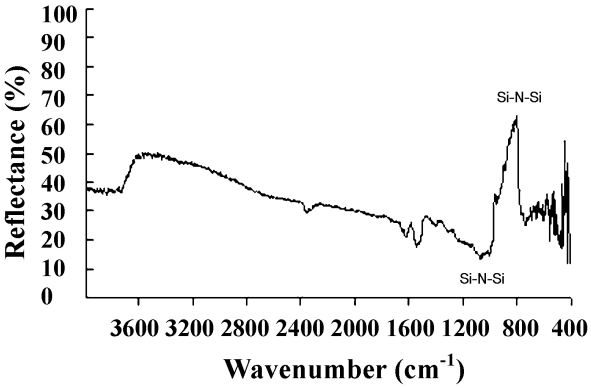

FIGURE 3. FT-IR spectrum corresponding to a specimen treated at a processing temperature and substrate temperature of 1173 K.

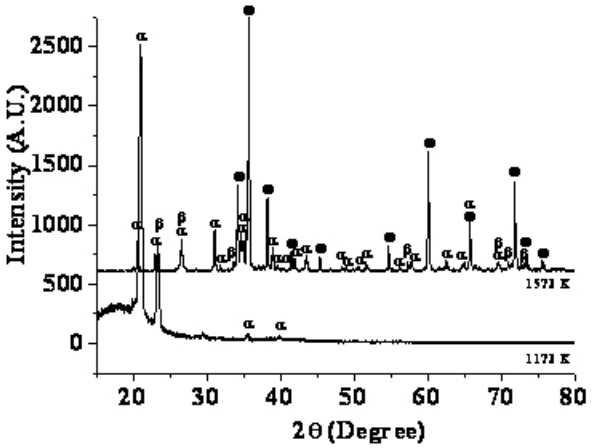

FIGURE 4. XRD patterns of specimens treated both at a processing temperature of 1573 K but while the first was studied at a substrate temperature of 1173 K, the second one at 1573 K. •corresponds to SiC, α and β represent α- and β-Si_3N_4, respectively.

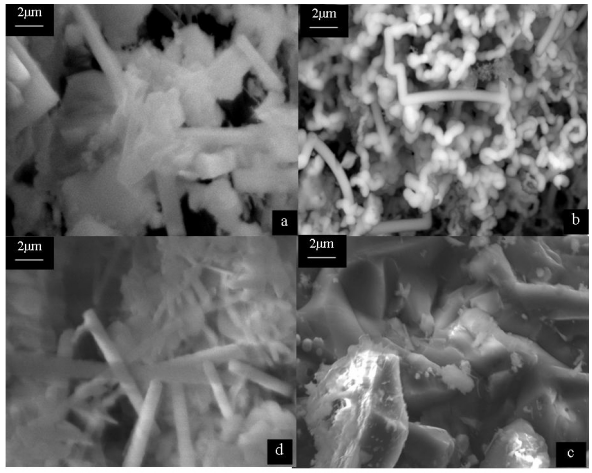

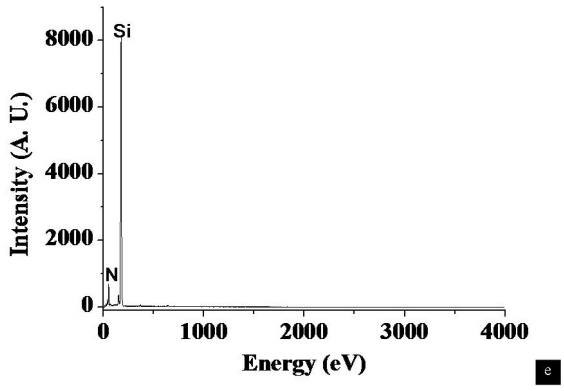

FIGURE 5. SEM photomicrographs showing Si_3N_4 deposited as: a) and b) whiskers, c), fibers d) coatings. e) Typical EDX spectrum obtained during analysis by SEM.

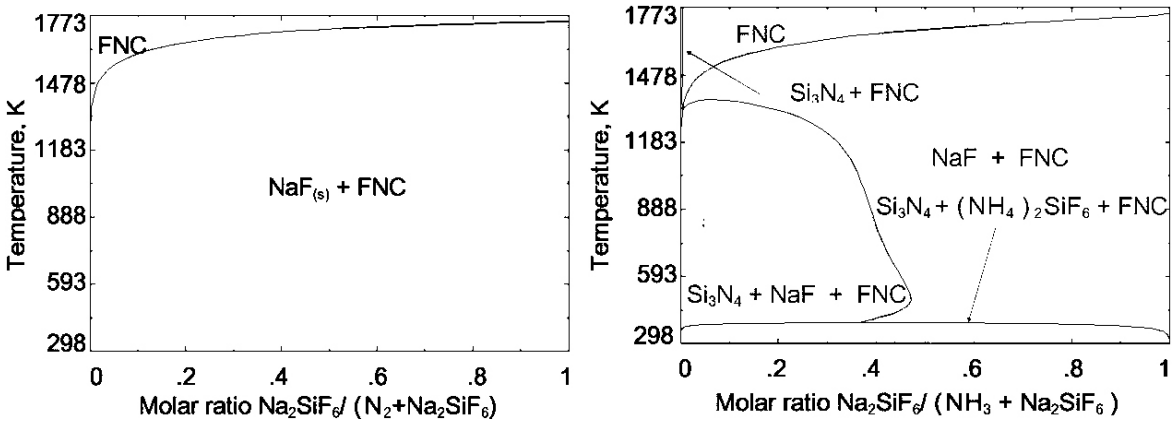

FIGURE 6. CVD phase diagram for (a) Na_2SiF_6-N_2 and (b) SiF_4-N_2 systems.

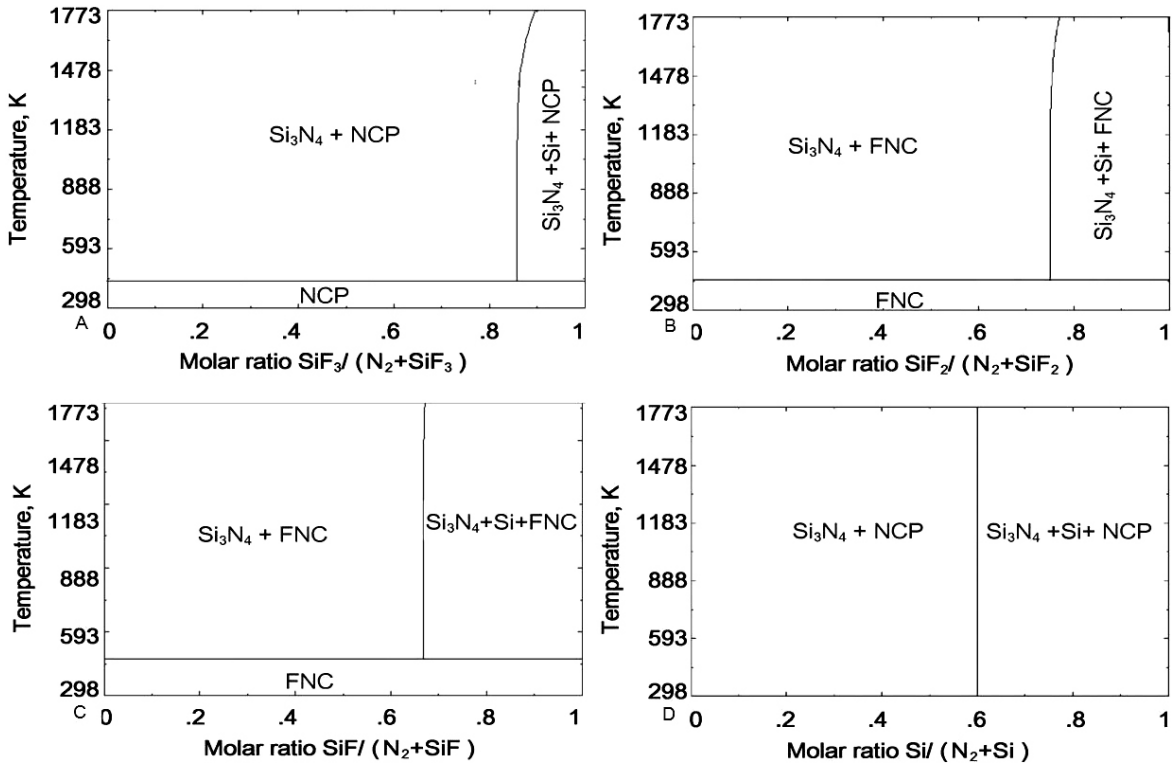

FIGURE 7. CVD phase diagrams for: (a) SiF_3-N_2, (b) SiF_2-N_2, (c) SiF-N_2 and, (d) Si-N_2 systems.

3.2. Microstructure characterization

In the case of specimens processed at low temperatures (below 1173 K), evidence of the Si-N-Si stretching mode at the characteristic wavenumber of 800-1200 cm^{-1} in FT-IR spectra suggests the presence of amorphous Si_3N_4in the as-deposited condition. The same wavelength range has been reported by several authors in the identification of Si-N-Si bonds, characteristic of silicon nitride [32-36]. Figure 3 shows the FT-IR spectrum of a specimen obtained at a substrate temperature of 1173 K (which also corresponds to the processing temperature). Conversely, above 1273 K analyses by X-ray diffraction indicate the formation of crystalline Si_3N_4. Figure 4 shows two diffractograms corresponding to specimens both of which were tested at a processing temperature of 1573 K. However, in the first specimen the substrate temperature was 1173 K while in the second the substrate temperature was 1573 K. The former shows the presence of a hump-like region characteristic of amorphous phases, and also some reflections of low intensity corresponding to α-Si_3N_4. The slight displacement in the α-Si_3N_4 peaks is associated with the transition from amorphous to crystalline sil-

icon nitride. The XRD pattern for 1573 K shows the presence of both α- and β-Si_3N_4. Moreover, results indicate that α-Si_3N_4 is formed predominantly at temperatures between 1273 and 1573 K while β-Si_3N_4 is produced only at the processing temperature of 1573 K. Analysis by SEM shows that Si_3N_4 can be deposited in a wide variety of morphologies including whiskers, fibers, coatings and powders (see Figs. 5a, 5b, 5c, and 5d). As shown in Fig. 5e, the presence of only silicon and nitrogen peaks in the EDX spectra confirms formation of crystalline Si_3N_4 by the synthesis route presented in this work.

3.3. Thermodynamic study and mechanism

Thermodynamic equilibrium predictions (see Figs. 6a and 6b) show that in the temperature range 294-1773 K it is not possible to deposit Si_3N_4 either from the SiF_4-N_2 system or through the Na_2SiF_6-N_2 system. In the former there is no condensed phase is obtained at all while in the latter the only solid reaction product is NaF. In the aforementioned phase diagrams the regions where only gas chemical species coexist are denoted as non-condensed phase (NCP) fields. Interestingly, in previous [12] and in current work (as was shown in the preceding section), fibers/whiskers, powders and coatings of α- and β-Si_3N_4 were obtained above 1273 K. This is in contrast with earlier studies on the synthesis of Si_3N_4 via CVD by feeding $SiF_{4(g)}$ and the nitrogen precursors (N_2 and NH_3) separately to the reactor, in which it was concluded that ammonia is preferred over pure nitrogen [26]. Thermodynamics also predicts that in the absence of the solids Na_2SiF_6 and NaF the direct gas phase reactions of SiF_4, SiF_3, SiF_2, SiF and Si with nitrogen lead to the formation of Si_3N_4 as a condensed phase (see Figs. 7a, 7b, 7c, and 7d). It should be noted that in all previous research into the thermal decomposition of Na_2SiF_6 it has simply been assumed that SiF_4 is the only gas reaction product (according to reaction (1)) [27-29]. Moreover, in no single report such an assumption ever been proven.

Equilibrium thermodynamic predictions show that, during the thermal decomposition of Na_2SiF_6 in nitrogen, the gas species SiF_3, SiF_2, SiF and Si are feasible in addition to SiF_4 and that at a given temperature the partial pressures of these chemical species increase with an increase in the F: Si ratio. Figure 8 shows plots of *log_{10}Pressure* vs. *temperature* for SiF_3, SiF_2, SiF and Si. From this figure it is evident that the SiF_3 chemical species appears at lower temperatures than the rest of the species and that at a fixed temperature it is the species with the highest partial pressure. These predictions together with the synthesis experimental results suggest that during the thermal decomposition of Na_2SiF_6 not only the SiF_4 species is produced but also - depending on the temperature- other reactive chemical species (SiF_3, SiF_2, SiF and Si) that facilitate the formation of Si_3N_4. It is also likely that the high F:Si ratio gas-species (mainly SiF_4) tend to further dissociate into lower F:Si ratio species. Hence, by the proposed route and in accordance with the arrangement of the Si precursor and the substrate within the reactor (see Fig. 1), Na_2SiF_6 works only as a silicon store in Zone I of the reactor in such a manner that as it decomposes, the produced gas species react with the flowing nitrogen in a high temperature region (Zone II) where only gas phase reactions take place, *i.e.*, where the Na_2SiF_6 and NaF solid phases do not intervene.

The argument on the thermodynamic unfeasibility for Si_3N_4 formation directly from $SiF_{4(g)}$ and pure nitrogen, and the possibility of synthesizing Si_3N_4 during the thermal decomposition of Na_2SiF_6in nitrogen (as in the current work) due to the evolution of other gas species with a lower F:Si ratio, can be reinforced by means of an analysis of energetic and thermochemical-stability aspects for SiF_4, SiF_3, SiF_2, SiF, Si and N_2. The main issue relates to the high energy required to dissociate the N_2 and SiF_4 precursors into more reactive species. According to previous calculations by others, the dissociation energy values for SiF_4 and nitrogen are 170 ± 10 [32] and 225.94 ± 0.14 kcal/mol [25], respectively, while those for SiF_3, SiF_2 and SiF are 118 ± 10, 153 ± 5 and 130 ± 3 kcal/mol, correspondingly. On the other hand, the heats of formation (ΔH_f^o) for SiF_4, SiF_3, SiF_2 and SiF, decrease in the following order: -386 $\pm$ 0.2, -235 $\pm$ 20, -136 $\pm$ 0.2 and -2 $\pm$ 3 kcal/mol, respectively [37]. Clearly since the SiF_3, SiF_2 and SiF species require less energy to dissociate than SiF_4 and N_2, their propensity to intervene in chemical reactions is higher. Moreover, they will dissociate up continuously and faster than $SiF_4$and N_2. These energetic and thermochemical parameters together suggest that, although more heat is evolved during SiF_4 formation, the lower dissociation energies for SiF_3, SiF_2 and SiF, represent a significant advantage in forming Si_3N_4. Also, because of its lower dissociation energy and by the partial pressure values shown in Fig. 8, it appears that SiF_3 is the gas species that most actively participates in the reaction for Si_3N_4 formation.

According to the above discussion, it is proposed that Na_2SiF_6 dissociates through a set of parallel and consecutive reactions that give place to other gaseous species in addition

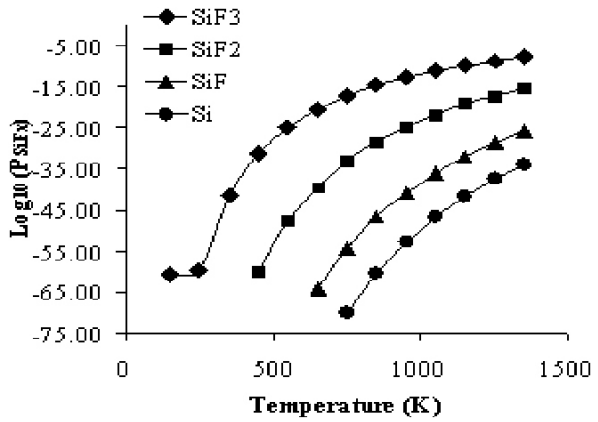

FIGURE 8. Equilibrium partial pressure (atm) of the silicon gas species (SiFx) formed from Na_2SiF_6 decomposition in nitrogen.

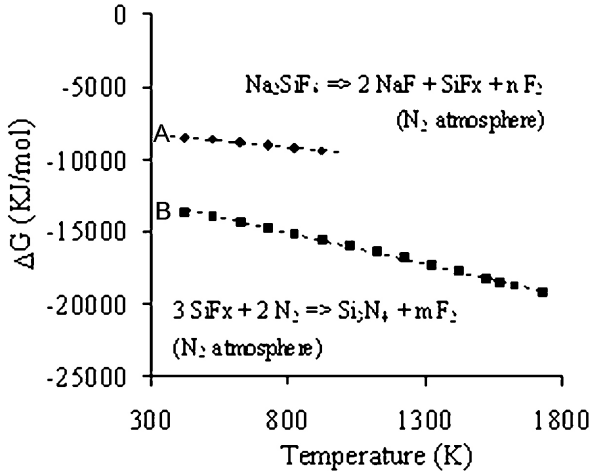

FIGURE 9. Ellingham diagrams for: a) decomposition of Na_2SiF_6 in nitrogen and, b) formation of silicon nitride from the reaction of SiF_x species with nitrogen.

to SiF_4 and that these species react with nitrogen to silicon produce nitride. Depending on the temperature, the parallel reactions produce directly the SiF_4, SiF_3, SiF_2, SiF and Si species while the consecutive ones consist of the subsequent dissociation of the species formed in the parallel events, *i.e.*, $SiF_4 \rightarrow SiF_3 \rightarrow SiF_2 \rightarrow SiF \rightarrow Si$. According to previous work, the decomposition of Na_2SiF_6 corresponds to a zero-order reaction with activation energy of 37.3 kcal/mol [30]. Details on the decomposition kinetics are reported elsewhere [30]. The overall decomposition reaction can be represented by:

$$5Na_2SiF_{6(s)} \rightarrow 10NaF_{(s)} + SiF_{4(g)} + SiF_{3(g)} + SiF_{2(g)} + SiF_{(g)} + Si_{(g)} + 5F_{2(g)} \quad (2)$$

$$\Delta G^o_{823K} = -2.20 \text{ kcal mol}^{-1}$$

Likewise, a mechanism for silicon nitride formation through the Na_2SiF_6-N_2 system is suggested. The highly reactive species (SiF_4, SiF_3, SiF_2, SiF and Si) generated from Na_2SiF_6 dissociation react with nitrogen to form Si_3N_4 as a stable solid phase by means of a set of parallel reactions. The total reactions can be summarized as follows:

$$3SiF_{4(g)} + 3SiF_{3(g)} + 3SiF_{2(g)} + 3SiF_{(g)} + 3Si_{(g)} + 10N_{2(g)} \rightarrow 5Si_3N_{4(s)} + 15F_{2(g)} \quad (3)$$

$$\Delta G^o_{1573K} = -4.41 \text{ kcal mol}^{-1}$$

Finally, the abridged reaction for synthesis of silicon nitride in nitrogen from the thermal decomposition of sodium hexafluorosilicate is:

$$3Na_2SiF_{6(s)} + 2N_{2(g)} \rightarrow Si_3N_{4(s)} + 6NaF_{(s)} + 6F_{2(g)} \quad (4)$$

It should be noted that both solid reaction products (Si_3N_4 and NaF) involved in reaction (4) were formed in the current work. However, due to the experimental arrangement they are located in different places within the reactor, *i.e.*, they are not mixed up. From the Ellingham diagrams corresponding to Na_2SiF_6 dissociation (in the temperature range 423-823 K) and Si_3N_4 formation (in the temperature range 423-1723 K), shown in Fig. 9, it can be confirmed that not only the feasibility for both reactions increases with temperature but also once the SiF_x species are formed, the reaction for Si_3N_4 formation is even more viable than that for Na_2SiF_6 dissociation.

4. Summary and conclusions

Si_3N_4 was successfully synthesized in a conventional CVD reactor from a hybrid precursor system ($Na_2SiF_{6(S)}$-$N_{2(g)}$). The process is based on the formation of Si-F gas chemical species (SiF_x) produced from the thermal dissociation of Na_2SiF_6in flowing nitrogen. While amorphous silicon nitride is formed between 1173 and 1273 K, α-Si_3N_4 and β-Si_3N_4 are produced in the temperature ranges 1273-1573K and above 1573K, respectively. Anova results show that pressure is the processing parameter that most significantly influences the formation of Si_3N_4, with a relative contribution of 35%, followed by processing temperature (32%) and time (32%). The optimum processing parameters to maximize the amount of silicon nitride in Na_2SiF_6-N_2 system are: 1573 K, 120 minutes and 17 mbars. The Na_2SiF_6dissociation mechanism in the temperature range from 423 to 823 K is represented by the following reaction:

$$5Na_2SiF_{6(s)} \rightarrow 10NaF_{(s)} + SiF_{4(g)} + SiF_{3(g)} + SiF_{2(g)} + SiF_{(g)} + Si_{(g)} + 5F_{2(g)} \quad (5)$$

And the Si_3N_4 formation mechanism in the temperature range from 473 to 1873 K is summarized through the following reaction:

$$3SiF_{4(g)} + 3SiF_{3(g)} + 3SiF_{2(g)} + 3SiF_{(g)} + 3Si_{(g)} + 10N_{2(g)} \rightarrow 5Si_3N_{4(s)} + 15F_{2(g)} \quad (6)$$

Although thermodynamics predicts the unfeasibility of synthesizing Si_3N_4 in the Na_2SiF_6-N_2 system, the proper arrangement of the silicon precursor and the substrates within the reactor, successfully enabled the production of Si-F gas species (apart from SiF_4) ready to react with nitrogen.

Acknowledgements

Authors express their gratitude to Conacyt (National council of Science and Technology, Mexico) for financial support under project No. CB-2005-1/24322. Dr. Leal-Cruz gratefully acknowledges Conacyt's assistance in providing a doctoral scholarship. Authors also wish to thank Mr. Felipe Marquez Torres for technical assistance during the characterization by scanning electron microscopy (SEM).

∗. Corresponding author. Phone: +52 (844) 438-9600 Ext. 9678. Fax: 438-9610, e-mail: martin.pech@cinvestav.edu.mx, martin_pech@yahoo.com.mx

1. F. Galasso, U. Kuntz, and W.J. Croft, *J. Am. Ceram. Soc.* **55** [8] (1972) 431.
2. K.S. Mazdiyasni and C.M. Cooke, *J.A. Ceram, Soc.* **56** [12] (1973) 628.
3. K. Hajime, S. Shinichi, and I. Takao, Japan Patent No. JP58115008 (1983).
4. W.-C. Lee and S.-L. Chung, *J. of Materials Research* **12** [3] (1997) 805.
5. K. Tang *et al.*, *Advanced Materials* **11** [8] (1999) 653.
6. A. de Pablos, J. Bermuda, and M.I. Osendi, *J. Am. Ceram. Soc.* **84** [5] (2001) 1033.
7. Y.G. Cao *et al.*, *J. of Crystal Growth* **234** (2002) 9.
8. C. Dianying, Z. Baolin, Z. Hanrui, L. Wenlan, and X. Suying, *Materials Research Bulletin* **37** |(2002) 1481.
9. H. Arik, *J. of the Eur. Cer. Soc.* **23** (2003) 2005.
10. Y. Gu, L. Chen, and Y. Qian, *J. Am. Ceram. Soc.* **87** [9] (2004) 1810.
11. I.G. Cano and M.A. Rodríguez, *Scripta Materialia* **50** (2004) 383.
12. A.L. Leal-Cruz and M.I. Pech-Canul, *Mater. Chem. and Phys.* **98** (2006) 27.
13. R.C.G. Swann, R.R. Mehta, and T.P. Cauge, *J. Electrochem. Soc.: Solid State Science.* **114** [7] (1967) 713.
14. E.A. Taft, *J. Electrochem. Soc.* **118** [8] (1971) 1341.
15. A.K. Sinha, H.J. Levinstein, T.E. Smith, G. Quintana, and S. E. Haszko, *J. Electrochem. Soc.: Solid-State Science and Technology* **125** [4] (1973) 601.
16. A.K. Sinha and T.E. Smith, *J. Appl. Phys.* **49** [5] (1978) 2756.
17. H. Nakayama and T. Enomoto, *Japanese J. of Appl. Phys.* **18** [9] (1979) 1773.
18. S. Fujita, M. Nishihara, W-L Hoi, and A. Sasaki, *Japanese J. of Appl. Phys.* **20** [5] (1981) 917.
19. M. Maeada and Y. Arita, *J. Appl. Phys.* **53** [10] (1982) 6852.
20. A.J. Lowe, M.J. Powell, and S.R. Elliot, *J. Appl. Phys.* **59** [4] (1986) 1251.
21. Y. Manabe and T. Mitsuyu, *J. Appl. Phys.* **66** [6] (1989) 2475.
22. R.K. Pandey, L.S. Patil, J.P. Bange, and D.K. Gautam, *Optical Materials* **27** (2004) 139.
23. W.E. Lee and W.M. Rainforth, *Ceramic microstructures*, property control by processing (Chapman & Hall, New York, 1994).
24. K.L. Choy, *Progress in Materials Science* **48** (2003) 57.
25. R.C. Weast, *C.R.C. Handbook of Chemistry and Physics*, 51 ed. (The Chemical Rubber Co., Cleveland OH, 1970).
26. F.S. Galasso, R.D. Veltri, and W.J. Croft, *Am. Ceram. Soc. Bull.* **57** [4] (1978) 453.
27. M. Vanka and J. Vachuška, *Termochimica Acta* **36** (1980) 387.
28. P. Chiotti, *Journal of Less-Common Metals* **80** (1981) 105.
29. Y. Kashiwaya and A.W. Cramb, *Metall. and Mater. Trans.* **33B** (2002) 129.
30. A.L. Leal-Cruz and M.I. Pech-Canul, *J. Solid State Ionics* **177** (2007) 3529.
31. R. Roy, *A Primer on the Taguchi Method, Society of Manufacturing Engineers* (Dearborn Michigan, 1990).
32. F.S. Galasso, R.D. Veltri, and W.J. Croft, *J. Amer. Ceram. Soc.* **57** [4] (1978) 453.
33. J.D. Wu *et al.*, *Thin Solid Films* **350** (1999) 101.
34. M. Vila, C. Prieto, P. Miranzo, M.I. Osendi, and R. Ramírez, *Surface and Coatings Tech.* **151-152** (2002) 67.
35. R.K. Pandey, L.S. Patil, Jaspal P. Bange, D.K., *J. Optical Materials* **27** (2004) 139.
36. B.S. Sahu, P. Srivastava, O.P. Agnihotri, and S.M. Shivaprasad, *J. of non-crystalline solids* **351** (2005) 771.
37. J.D. McDonald, C.H. Williams, J.C. Thompson, and J.L. Margrave, *Advan. Chem. Ser.* **72** (1968) 261.